

Morphological Characterization of Polyetheretherketone-Carbon Fiber Composites

C. M. TUNG and P. J. DYNES,* *Rockwell International Science Center, Thousand Oaks, California 91360*

Synopsis

The effect of processing conditions on the morphology of polyetheretherketone (PEEK) graphite reinforced composites (APC-2) has been characterized. Differential scanning calorimetry was utilized to examine the effect of quench rate on recrystallization where a change in mechanism was observed at a rate of 5°C/min. Optical microscopy revealed a decrease in spherulite size and a reduced degree of transcrystallinity at the graphite fiber surface with increasing quench rates. Dynamic mechanical analysis indicated a change in relaxational processes in the T_g region with varying quench rates.

INTRODUCTION

Polyetheretherketone (PEEK) is one of the emerging thermoplastic materials that has become particularly attractive for advanced composite applications. It offers fracture toughness and delamination resistance that are an order of magnitude greater than state-of-the-art epoxy-based composites. The outstanding solvent and moisture resistance remove one of the major stumbling blocks to the utilization of thermoplastics in aircraft structural applications. In addition, the processing flexibility enables potential adaptation to high rate production processes, thus reducing manufacturing costs. A critical issue in the processing of a semicrystalline material such as PEEK is the microstructure or morphology of that material. Morphological features such as degree of crystallinity, spherulite size, lamellae thickness, and crystallite orientation have a profound impact on the ultimate properties of the polymer. These features are, in turn, affected by the variation in the processing conditions. To obtain a clear understanding of the processing-morphology-property relationships in PEEK, the morphological changes that occur during processing must be monitored so that critical processing parameters can be identified. The crystallization behavior of PEEK under isothermal conditions was reported by Blundell and Osborn.¹ Recently, assessment of crystallinity of graphite-reinforced PEEK composites (APC-2) was described independently by Blundell et al.² and James and Anderson.³ In this paper, we present results on morphological characterization of PEEK composites (APC-2) processed under nonisothermal conditions. The morphological characterization was carried out by monitoring the crystallization and melting behavior, degree of crystallinity, spherulite size, orientation, and the dynamic mechanical responses as functions of processing conditions. A combination of tech-

*Present address: Northrop Aircraft, Hawthorne, CA.

niques such as differential scanning calorimetry (DSC), transmission optical microscopy, and dynamic mechanical spectroscopy were employed to provide insights into the morphology of PEEK composites during processing.

EXPERIMENTAL

Material

APC-2, one of the Aromatic Polymer Composites supplied by Imperial Chemical Industries, (ICI), was bag-molded by North American Aircraft Operations (NAAO) of Rockwell International using a gas pressure consolidation technique for this study. This material contains Hercules AS4 graphite fiber impregnated with poly(etheretherketone) (Vicat PEEK)[†] which has a melting point of 345°C.

Sample Preparation

To prepare quenched samples for the microscopic and dynamic mechanical studies, the laminates were first heated in a programmable press at 400°C for 10–15 min and then quenched at different rates. The cooling rates were controlled in the following fashion:

1. The slow cooling rates of 1.5 and 5°C/min were controlled by the temperature programmer of the press.

2. The faster cooling rate of ~ 70°C/min was obtained by transferring the sample from a heated press to a cold press of which the platen temperature was maintained by the circulating water.

3. The very fast cooling rate of ~ 2500°C/min was achieved by immersing the heated sample into liquid nitrogen. The rate was estimated based on the time required to remove the heated sample from the programmable press to liquid nitrogen bath. There was no thermocouple embedded in the sample.

The samples were microtomed into sections of approximately 8 μm thickness and examined by polarized optical microscopy. Dynamic mechanical measurements were made using the dynamic torsion rectangular mode of Rheometrics Dynamic Spectrometer at a frequency of 10 rad/s. The torsion specimen was a rectangular bar ~ 7 cm long, 1.2 cm wide, and 0.2 cm thick with the fibers parallel to the long dimension. For DSC studies, the Perkin-Elmer DSC-2 was used to characterize thermal behavior with samples heated at 400°C for 10–15 min and then quenched at controlled rates in the sample holder. For extremely fast quenching [Fig. 3(b)], samples were first melted in an enclosed DSC pan in the sample holder and then dipped into dry ice.

RESULTS AND DISCUSSIONS

Crystallization Behavior

The effect of quench rate on the crystallization exotherms of APC-2 is shown in Figure 1, where a higher rate lowers T_{cm} (the temperature at which the maximum rate of crystallization from the melt is obtained). The depen-

[†]The trademark of Imperial Chemical Industries PLC.

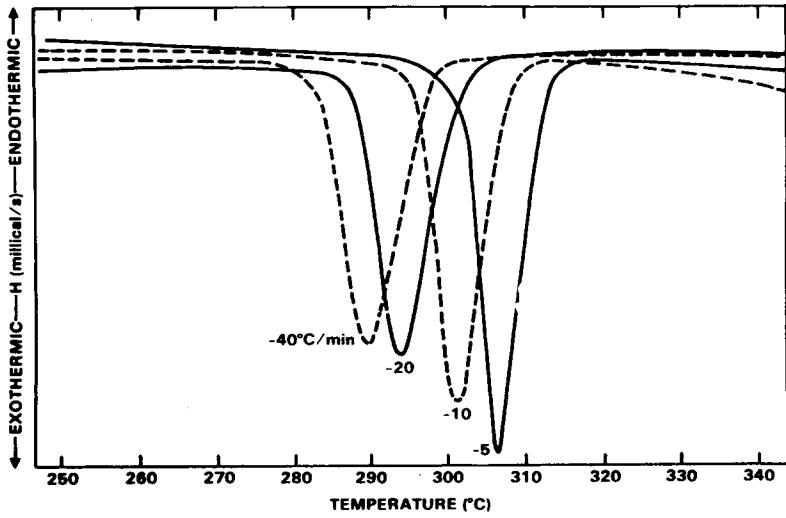


Fig. 1. DSC thermograms of crystallization in the melt state for APC-2 at various quench rates.

dence of T_{cm} with quench rate can be described by a modified expression as shown in Figure 2,

$$E_a = - \frac{Rd \ln \Phi}{1.052d(1/T_{cm})} \tag{1}$$

where Φ is the quench rate and R is the gas constant.⁴ A change in slope is observed with the transition occurring at a cooling rate of approximately 5°C/min. The calculated activation energy is about 115 kcal/mol for the slow

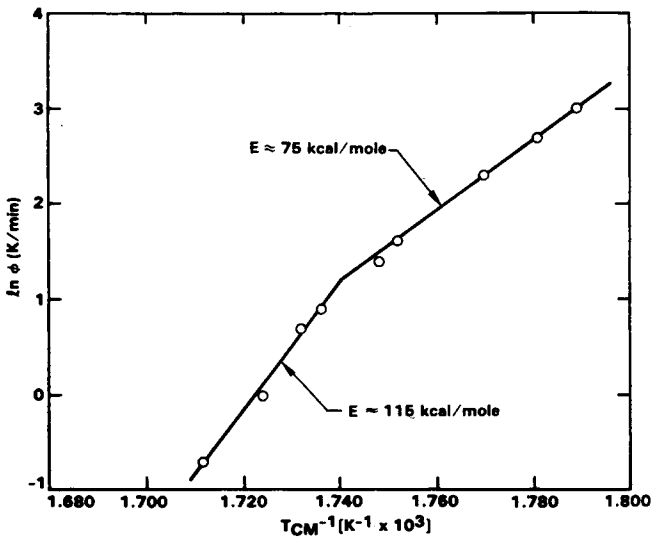


Fig. 2. Effect of quench rate on T_{CM} of APC-2.

quench rates and 75 kcal/mol for the fast rates, suggesting a change in mechanism of crystallization for PEEK.

Recently, a paper by Blundell and Osborn⁵ also reported a continuous decrease in the T_{cm} of APC-2 as the quench rate increases. Based on a model using the Avrami kinetic equation, they further predicted that the T_{cm} would reach a steady value of about 210°C when the cooling rate is in excess of 1000°C/min.

Melting Behavior

The crystallization of PEEK can also be studied by analyzing the melting behavior of the crystalline phase. When APC-2 [Fig. 3(a)] was cooled at slow rates such as 0.5, 1, 2.5°C/min, etc., a pronounced initial low melting endotherm that is lower in temperature than that of the major melting endotherm was observed. On the other hand, an exothermic crystallization peak was observed for samples quenched at a very fast quench rate [Fig. 3(b)].

This initial low melting endotherm is shifted toward a higher temperature and increased in size with decreasing quench rates. This double melting behavior can be explained in terms of the recrystallization hypothesis put forward by Holdsworth and Turner-Jones.⁶ They argued that the low melting peak is associated with the melting of the crystalline regions formed during the previous quenching. The location of this initial peak, therefore, is de-

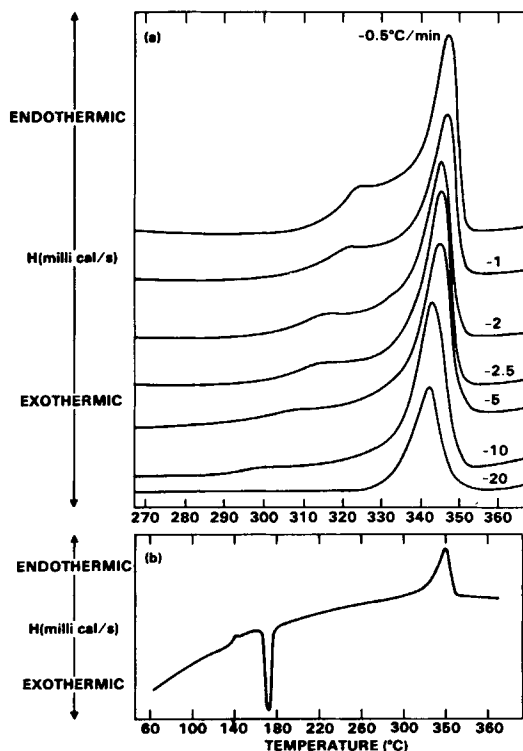


Fig. 3. DSC thermograms of the melting behavior of APC-2 cooled at various rates: (a) Slower than 20°C/min; (b) very fast quenching.

terminated by the microstructure of the imperfect crystallites formed by the quenching process and is a function of the quench rate. The higher the quench rate, the lower the initial melting temperature will be. When these low-melting crystallites are melted during the subsequent DSC scan, recrystallization occurs. Therefore, the final melting peak represents the net result of these two processes and is characteristic of the best crystalline structure attainable under the experimental conditions.

The emergence of a second low melting peak in the DSC thermograms of samples quenched at slow rates could suggest a change in crystallization mechanism of APC-2. Lin and Koenig⁷⁻⁹ carried out a series of DSC studies on the isothermal crystallization of poly(ethylene terephthalate) (PET). In those studies, they reported that when samples were annealed above a certain temperature, a transition from an exothermic crystallization peak to an endothermic low melting peak was observed in the DSC thermograms. The endothermic low melting peak initially is weak and increases in size and moves to higher temperature with increasing time of annealing. Based on the results of Fourier transform infrared spectroscopy (FTIR) and density measurements, they concluded that a change in crystallization mechanism occurs at the time of transition. The similarity in the melting behavior of PET and PEEK resin in APC-2 suggests that analogous changes probably also occur in the nonisothermal crystallization of PEEK. At high quench rates, very little time is allowed for small crystallites to grow in size and perfection. PEEK resin probably undergoes certain structural and morphological changes such as reorganization of amorphous regions through chain transport, crystallization of amorphous chain segments, and the rejection of defects from crystals. The DSC thermograms of those samples are characterized by an exothermic crystallization peak and a major melting peak. At slow quench rates, small crystallites are allowed to develop into crystalline blocks of increased size and perfection. Those crystals undergo melting and recrystallization processes to form more perfect and larger crystals during the DSC scan. The transition from the stage of reorganization of amorphous region to that of perfection of crystalline blocks probably occurs somewhere between the quench rates of 5 and 10°C/min as is evident from the emergence of the low melting peak. The structural rearrangement involved in the latter transformation step requires a larger amount of energy,⁸ as indicated by the higher activation energy (115 kcal/mol) measured for PEEK resin quenched at slower rates ($\leq 5^\circ\text{C}/\text{min}$) as compared with that of resins quenched at faster rates (75 kcal/mol).

Transmission Optical Microscopy

To establish sound morphology-processing relationships, direct means to monitor morphological changes during processing must be employed. The birefringent nature of the spherulites enables them to be readily visible using an electron or a polarized optical microscope. Thus far, the only published optical microscopy data on the morphology of PEEK are those by Cogswell¹⁰ and Blundell and Osborn.¹ The micrographs of Cogswell show spherulitic structure in PEEK neat resin with a very fine texture. A similar result was reported by Blundell and Osborn¹ for neat resin in which such a fine pattern was obtained. They were able, however, to obtain a sample with a

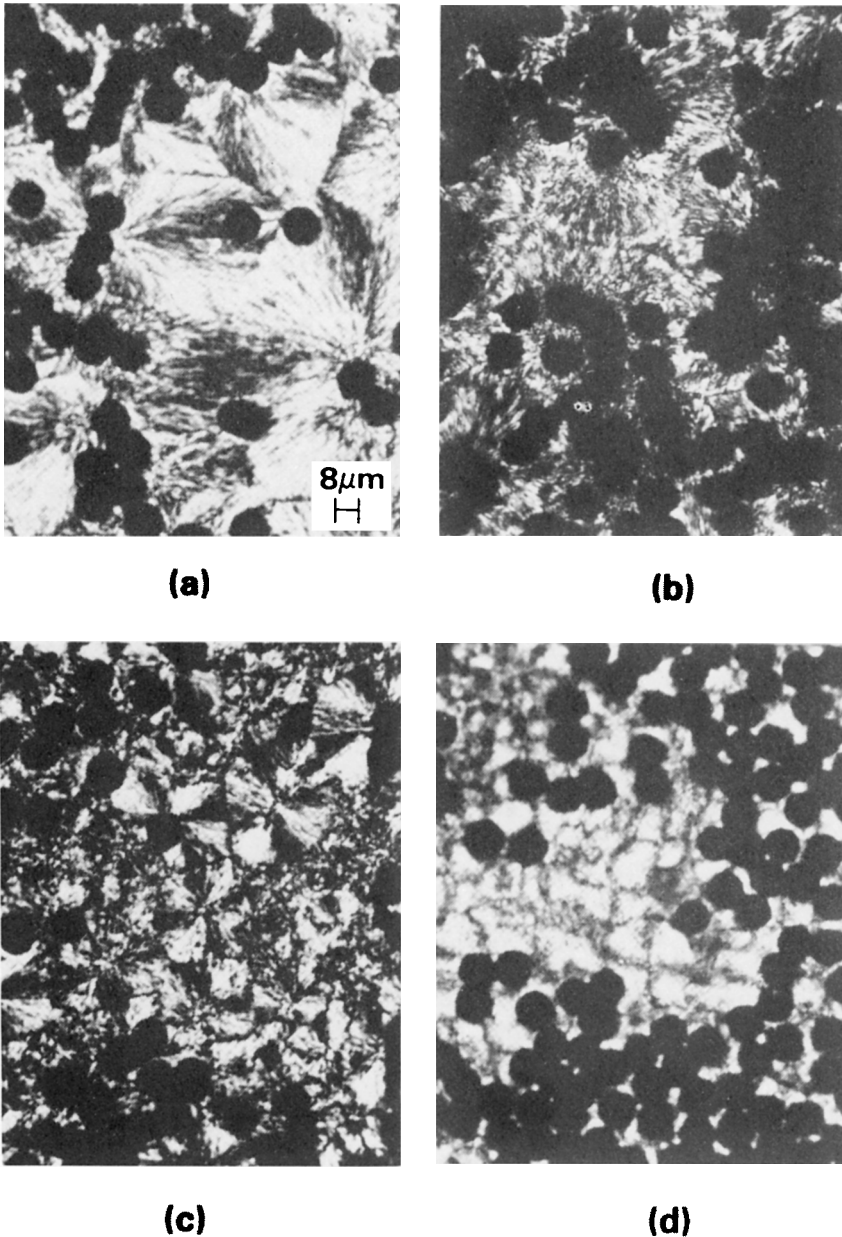


Fig. 4. Effect of quench rate on spherulite size of APC-2: (a) 1.5°C/min; (b) 5°C/min; (c) 70°C/min; (d) 2500°C/min.

lower nucleation density in which to grow larger spherulites. The effect of quench rate on the final spherulite size is shown in Figure 4.

Slow quenching such as 1.5 and 5°C/min produced spherulites with the respective radii around 25 and 15 μm, a result similar to that reported by Christensen and Clark.¹¹ Faster quenching (~70°C/min) produced spherulites of half the size ($r = 10 \mu\text{m}$); very fast quenching ($\approx 2500^\circ\text{C}/\text{min}$)

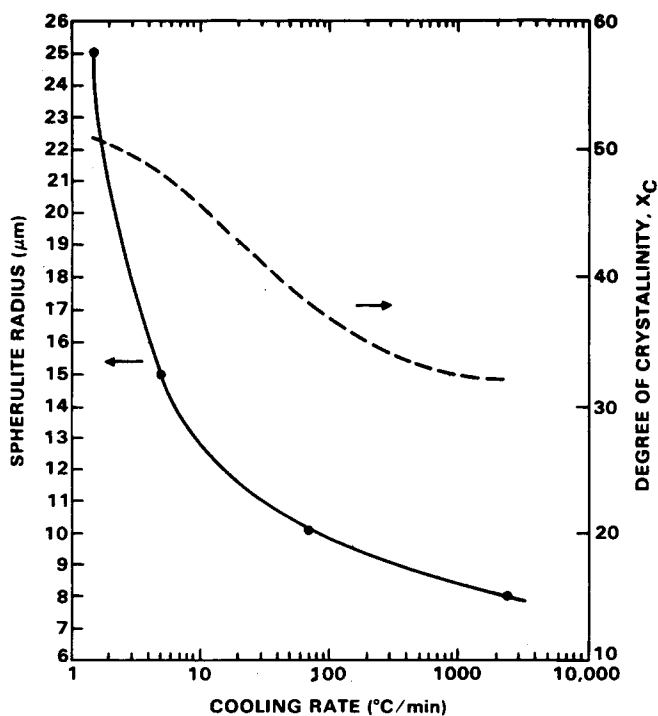


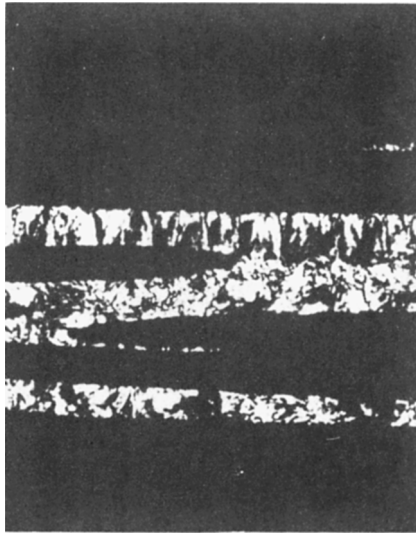
Fig. 5. Effect of quench rate on spherulite size and degree of crystallinity.

produced spherulites with radii around $8 \mu\text{m}$. The decrease in the spherulite size with increasing quench rates is plotted in Figure 5. The rapid increase in spherulite size at slower quench rates ($\leq 10^\circ\text{C}/\text{min}$) is probably due to the decrease in the number of nucleation sites, as faster quench rates are known to produce greater numbers of spherulites.¹² The trend in the change of spherulite size as a function of quench rate parallels the degree of crystallinity measurements obtained by wide-angle X-ray technique (Fig. 5),³ although the decrease in crystallinity is probably due to the incomplete growth of spherulite at fast quench rates.⁵

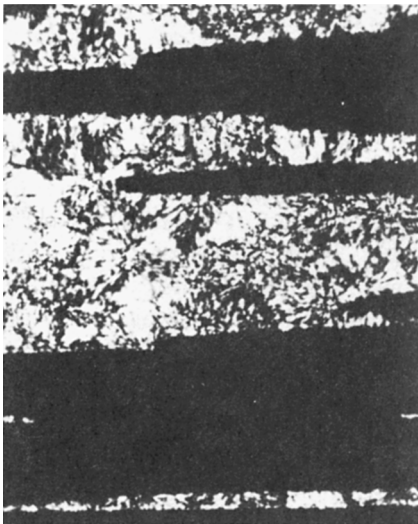
Quench rates also appear to affect the formation of transcrystalline regions where the crystals nucleate perpendicular to the reinforcing fibers. The development of transcrystallinity is quite noticeable in slow-cooled samples [Fig. 6(a)], while not very apparent in the fast-cooled samples [Figs. 6(b) and 6(c)]. The formation of transcrystallinity enhances fiber/matrix bonding, but may have a detrimental effect on the long-term composite strength.¹³ It is therefore critical to identify the processing parameters, which might lead to such a detrimental orientation effect.

Dynamic Mechanical Spectroscopy

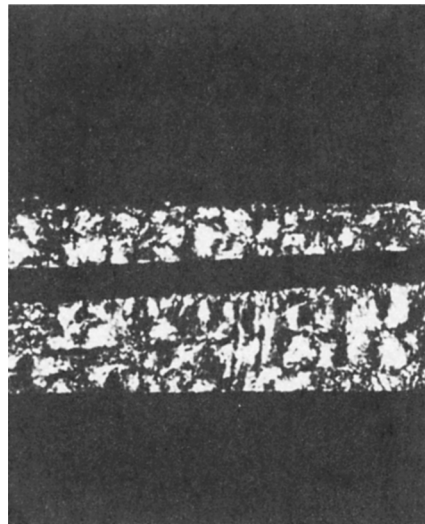
Dynamic mechanical measurements have been extensively used to study the relaxation processes in polymers. The intensity and temperature of the glass transition were shown to be affected by subtle changes in crystalline morphology or supermolecular structure of certain polymers.¹⁴ The impact



(a)



(b)



(c)

Fig. 6. Development of transcrystallinity in APC-2 cooled at various rates: (a) 1.5°C/min; (b) 70°C/min; (c) 2500°C/min.

strength,¹⁵ creep, and stress-relaxation^{15,16} properties of glassy polymers have also been associated with the main chain low temperature relaxation processes. In the present study, the effect of thermal history on the dynamic mechanical responses, such as storage modulus (G'), loss modulus (G''), and loss tangent ($\tan \delta$) were examined over the temperature range from -120°C to 350°C . A typical spectrum is shown in Figure 7. The value of G' remains nearly constant from -120°C to near T_g ($\approx 150^\circ\text{C}$). The modulus then decreases by

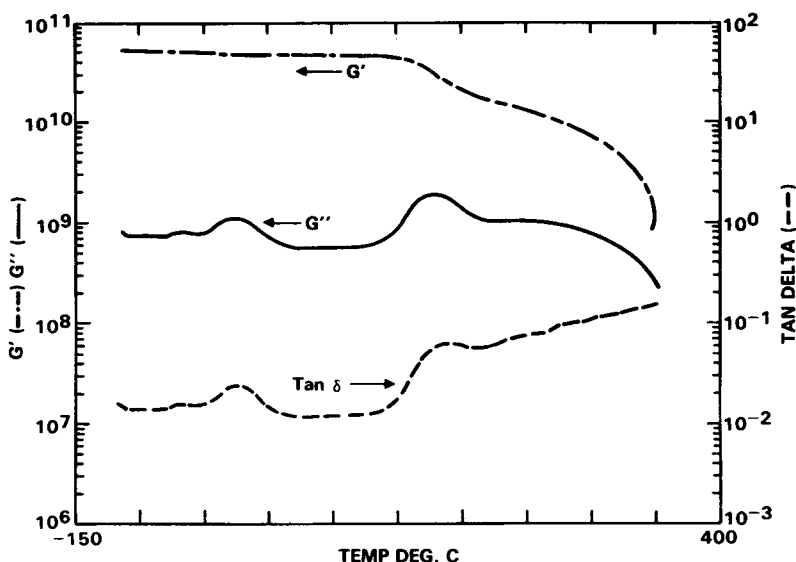


Fig. 7. Schematic of a dynamic mechanical spectrum of APC-2.

about an order of magnitude until the melting temperature T_m is approached. The G'' vs. T and $\tan \delta$ vs. T curves reveal several low-temperature transition peaks that may represent different relaxation processes in the glassy region. The intensities and locations of the transition peaks, as well as their frequency-temperature behavior, were monitored as functions of the processing conditions. The objective was to explore the usefulness of dynamic mechanical spectroscopy as a possible technique to characterize the crystalline morphology of thermoplastic composites.

Effect of Processing on G'

The effect of processing conditions on the storage modulus of APC-2 composites is shown in Figure 8, where the modulus-temperature curves of samples quenched at different rates are plotted over a temperature range of 80–350°C. The steepness of the curves seems to correlate with the processing conditions; i.e., the faster the quench rate, the steeper the slope becomes. The rubbery state modulus of the sample quenched at a fast rate is also slightly lower than that of the samples quenched at slower rates of 1.5, 5, or 70°C/min. The data infer that samples quenched at the fastest rate possess greater molecular mobility in the glass transition region than the samples quenched at slow rates. This can be explained in terms of increased free volume as well as decreased degree of crystallinity in the fast-quenched sample. A very fast quench rate results in greater free volume and hence imparts greater mobility to the polymeric backbone. A lowering of the degree of crystallinity in these samples can also produce the same effect. A simple model proposed by Boyer¹⁷ (Fig. 9) illustrates this point. In a semicrystalline material, the polymer chain comprises a crystalline-amorphous sequence involving a constant number $N^* = N_c + N_a$, of carbon atoms. The strength of each relaxation is proportional to the number of carbon atoms involved. In the

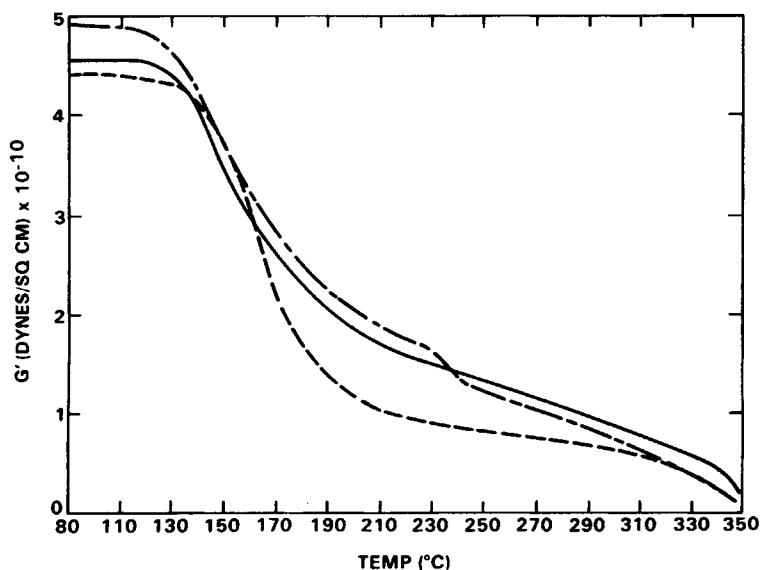


Fig. 8. Effect of processing on storage modulus (G') of APC-2: (—) 1.5, 70°C/min; (---) 5°C/min; (-·-) 2500°C/min.

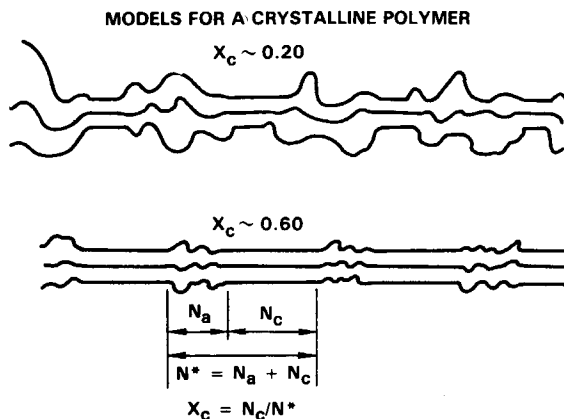


Fig. 9. Crystallization model as proposed by Boyer.

glass transition region, the number of carbon atoms in the amorphous region (N_a) determines the relaxation strength and thus mobility of the macromolecules. Lower crystallinity produces relatively greater mobility and, hence, the steeper slope of the modulus-temperature curve. The steepness of the modulus-temperature curve can therefore be correlated to the degree of crystallinity. An analogous conclusion was reached for crosslink density in a thermoset system,¹⁸ in which the steepness of modulus-temperature curve was also found to be a function of crosslink density.

Effect of Processing on the G'' and $\tan \delta$ Loss Peaks

Several loss peaks can be seen to appear in the same temperature region in the G'' vs. T and $\tan \delta$ vs. T curves. The loss peak of the highest temperature

TABLE I
Glass Transition Temperature for Samples Quenched at Different Rates

| Quench rate (°C/min) | Temperature of maximum $G''/\tan \delta$ (°C) |
|-------------------------|--|
| 1.5 | 154/163 |
| 5 | 150/159 |
| 70 | 154/164 |
| 2500 | 160/171 |

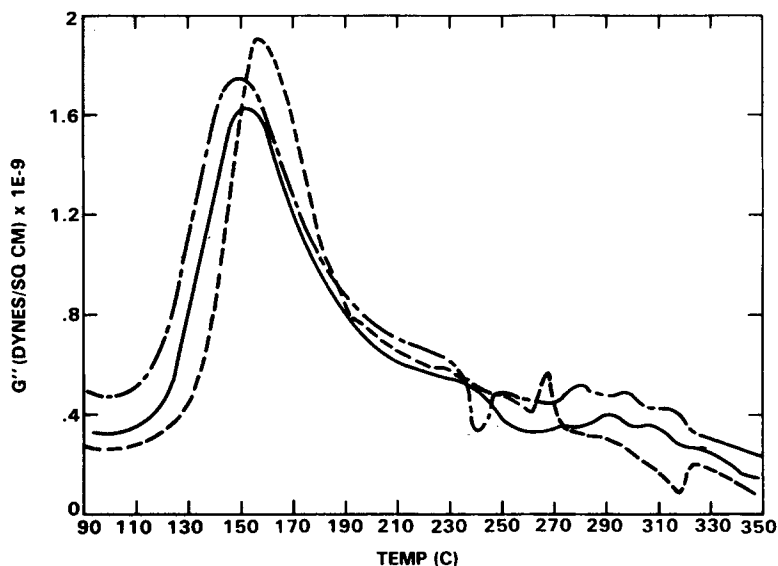


Fig. 10. Effect of processing on loss modulus (G'') of APC-2 at T_g : (—) 1.5°C/min; (---) 5°C/min; (-·-) 2500°C/min.

is associated with the main glass transition (T_g transition) and the multiple low temperature loss peaks are associated with secondary glass transitions ($T < T_g$ transition). Although they represent the same relaxation processes, peak maxima in $\tan \delta$ vs. T curves appear at higher temperatures than those in G'' vs. T curves (Table I). This is usually true for polymers having a wide range of relaxation times. Because the peak shape in the G'' vs. T curve are better defined, its positions will be used for the following discussion.

The effect of processing on T_g and $T < T_g$ transitions is shown in Figures 10 and 11. The loss peaks in the T_g transition region are shown to be sensitive to the changes in processing conditions, which in turn are sensitive to the crystallinity of different samples. A plot of G''_{\max} as a function of crystallinity is shown in Figure 12. G''_{\max} shows a rapid decrease as the degree of crystallinity (X_c) increases from 0.32 to 0.59. The decline levels off after X_c reaches 0.38.

A slight increase in T_g is observed as the quench rate increases from slow to very fast. The shift is unexpected as the glass transition temperature is intimately related to the free volume. T_g is expected to decrease as the rate of cooling from the melt increases.¹⁹ The exact cause of this shift is unclear at

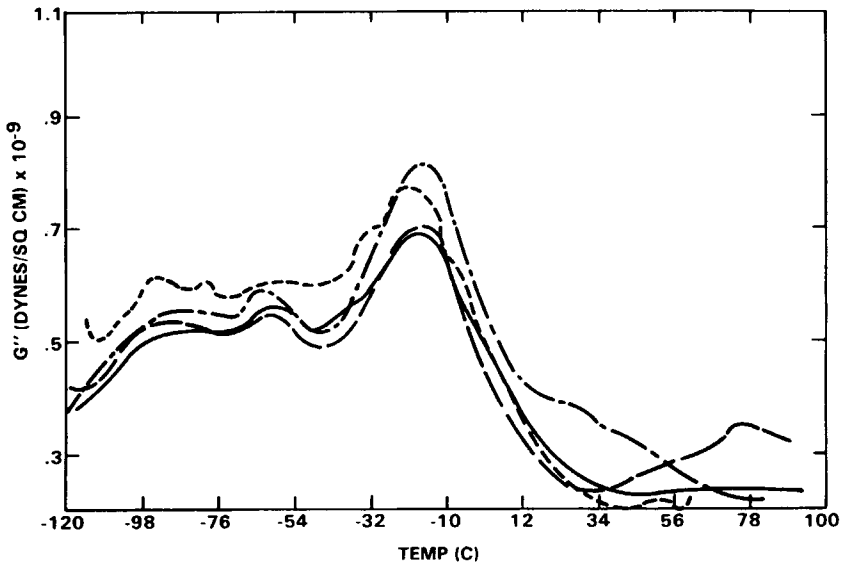


Fig. 11. Effect of processing on loss modulus (G'') of APC-2 at $T < T_g$: (—) 1.5°C/min; (---) 5°C/min; (- -) 70°C/min; (- · -) 2500°C/min.

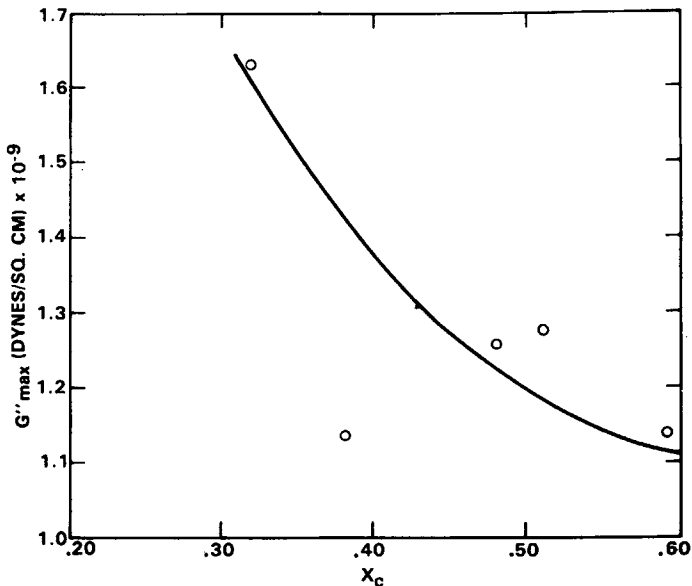


Fig. 12. Plot of G''_{\max} as a function of degree of crystallinity (X_c) of APC-2 at T_g .

the moment. A possible explanation is that the rapid cooling may cause closer packing as a result of large temperature gradient across the sample. This type of shrinkage may cause a shift to higher T_g .

The loss peaks in the lower temperature ($T < T_g$) transitions appear to be less sensitive to variation in processing. The G''_{\max} vs. X_c curve, as illustrated in Figure 13, shows little correlation between G''_{\max} and X_c . This is expected,

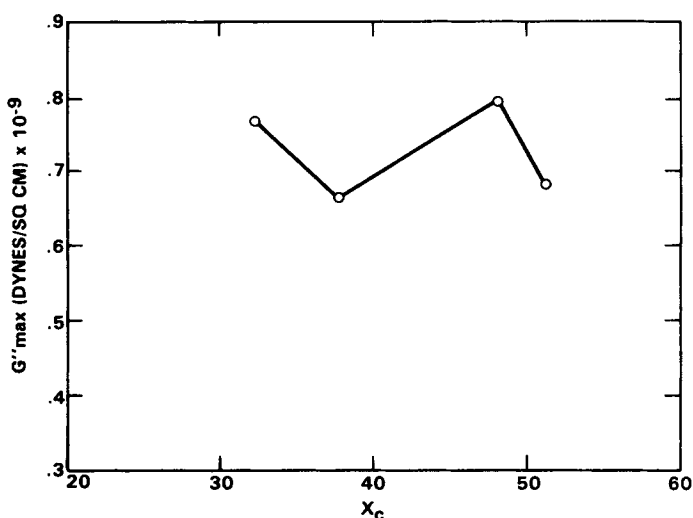


Fig. 13. Plot of G''_{\max} as a function of degree of crystallinity (X_c) of APC-2 at $T < T_g$.

as those transitions probably involve only the movement of short-chain segments in a polymer chain. The appearance and magnitude of those transitions, nevertheless, may shed light on the mechanical properties, such as impact strength, creep, and stress-relaxation properties of glassy polymers.

The Effect of Processing on the Frequency-Temperature Dependence of Dynamic Mechanical Properties

The frequency-temperature dependence of the dynamic mechanical properties was studied by examining the shift of T_g and $T < T_g$ transitions as frequency was stepwise increased from 1 to 100 cycles/s. As evident from Figure 14, the transition temperatures follow an Arrhenius relation:

$$\ln f = -\frac{E_a}{RT_{\max}} + c \quad (2)$$

where E_a is the apparent activation energy, R is the gas constant, T_{\max} is the absolute temperature for the transition, and c is a constant. From the slopes of the straight lines the activation energies for T_g and the $T < T_g$ transitions were estimated. The result is shown in Table II. As expected, the activation energy for T_g transition is much higher than that for $T < T_g$ transition, consistent with the assumption that $T < T_g$ transition involves only local chain movement. Very little difference, however, is seen in the E_a of both T_g and $T < T_g$ transitions as a result of different processing conditions. One possible explanation is that the simple Arrhenius expression may not entirely describe the frequency temperature dependence of those systems. An alternative way to describe the temperature-frequency behavior is to use the William-Landel-Ferry (WLF) approach, where the master curve of each processed material is obtained by shifting spectra over a frequency range of 1-10 rad/s.

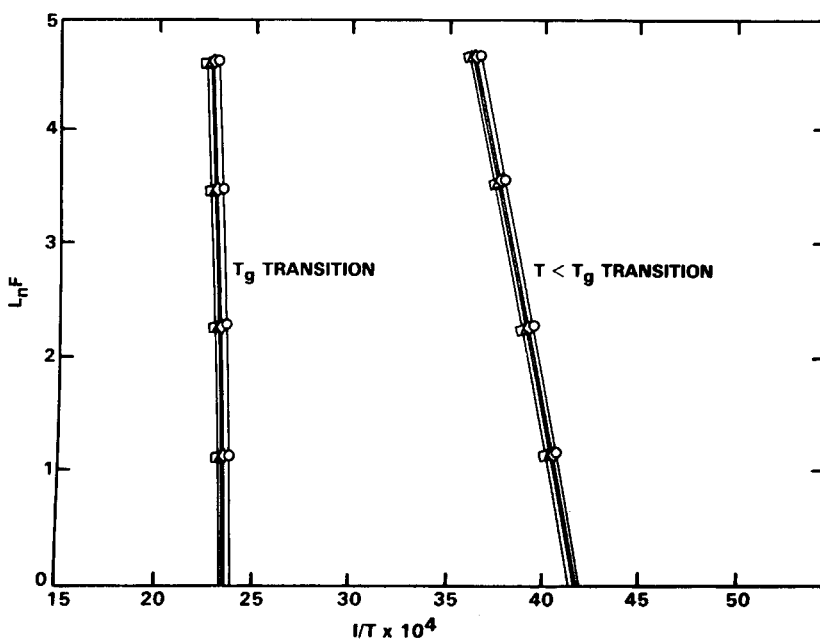


Fig. 14. Frequency-temperature correlation plot for APC-2 quenched at different rates: (Δ) 1.5°C/min; (\circ) 5°C/min; (\diamond) 70°C/min; (\square) 2500°C/min.

TABLE II
Activation Energies of T_g and $T < T_g$ Transitions

| Quench rate (°C/min) | $E_a(T_g)^a$ (kcal/mol) | $E_a(T < T_g)$ (kcal/mol) |
|-------------------------|----------------------------|------------------------------|
| 1.5 | 166 | |
| 5 | 157 | ~ 22 |
| 70 | 159 | |
| 2500 | 180 | |

^aStandard of deviation is $\sim \pm 10\%$.

The results are shown in Figure 15, where the modulus-frequency behavior at the reference temperature, $T_0 = 160^\circ\text{C}$, is obtained for the three quenched materials. It is apparent from those curves that the effect of processing is most evident in the low frequency region where the polymers are in the rubbery state. The low modulus of the very fast quenched sample (quench rate = 2500°C/min) correlates well with lower degree of crystallinity in this sample. The effect of processing is not so obvious in the high frequency region where the polymers are in the glassy state.

CONCLUSIONS

The effect of processing on the morphology of PEEK APC-2 composites is clearly demonstrated. Two-stage crystallization process was seen in samples quenched at slow rates ($< 5^\circ\text{C}/\text{min}$). Crystallinity, spherulite size, and orientation were also affected by the quenched rates, with high crystallinity, large

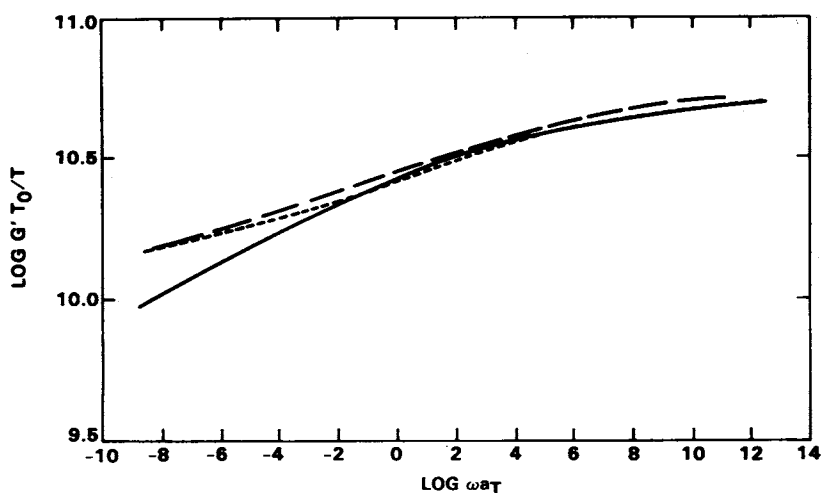


Fig. 15. Master curves of APC-2 quenched at different rates ($T_0 = 160^\circ\text{C}$): (---) $1.5^\circ\text{C}/\text{min}$; (-·-) $70^\circ\text{C}/\text{min}$; (—) $2500^\circ\text{C}/\text{min}$.

spherulites, and transcrystallinity being observed in very slow quenched samples. The slope of the modulus-temperature curve and the intensity of the loss modulus in the glass transition region were found to be sensitive to the various cooling rates. Little effect of processing was seen on the relaxation processes in the $T < T_g$ region. Processing also appeared to affect the shear storage modulus of the polymers in the rubbery state while little effect was observed in the glassy polymers.

The research was sponsored by the Science Center, Rockwell International, under Independent Research and Development. The authors wish to acknowledge Mr. C. Mauthe for his assistance in obtaining the microscopic data and Dr. A. Yang of NAAO for supplying APC-2 samples. The authors are also grateful to Drs. C. Leung and R. Morgan for helpful discussions during the course of this work.

References

1. D. J. Blundell and B. N. Osborn, *Polymer*, **24**, 953 (1983).
2. D. J. Blundell, J. M. Chalmers, M. W. MacKenzie, and W. F. Gaskin, *SAMPE Q.*, **16**, 22 (1985).
3. M. R. James and D. P. Anderson, *Adv. X-Ray Anal.*, **29**, (1985).
4. A. A. Duswalt, *Thermo Chem. Acta.*, **8**, 56 (1974).
5. D. J. Blundell and B. N. Osborn, *SAMPE Q.*, **17**, 1 (1985).
6. P. J. Holdsworth and A. Turner-Jones, *Polymer*, **12**, 195 (1974).
7. S. B. Lin and J. L. Koenig, *J. Polym. Sci., Polym. Phys. Ed.*, **21**, 2277 (1983).
8. S. B. Lin and J. L. Koenig, *J. Polym. Sci., Polym. Phys. Ed.*, **21**, 2365 (1983).
9. S. B. Lin and J. L. Koenig, *J. Polym. Sci., Polym. Symp.*, **71**, 121 (1984).
10. F. N. Cogswell, *Proc. 28th Natl. SAMPE Symp.*, 528 (1983).
11. S. Christensen and L. P. Clark, "Thermoplastic Composite Technology Development," F33615-83-C-5011, Interim Report No. 5.
12. W. Banks, J. N. Hay, A. Sharples, and G. Thompson, *Polymer*, **5**, 163 (1964).

13. A. Lustiger, *SAMPE J.*, **20**, 13 (1984).
14. L. Mandelkern, M. Glotin, R. Popli, and R. S. Benson, *J. Polym. Sci., Polym. Lett. Ed.*, **19**, 435 (1981).
15. R. Buchdahl and L. E. Nielsen, *J. Appl. Phys.*, **21**, 482 (1950).
16. K. C. Rusch, *J. Macromol. Sci.-Phys.*, **B2**, 179 (1968).
17. R. F. Boyer, *J. Polym. Sci. Symp.*, **50**, 189 (1975).
18. T. K. Kwei, *J. Polym. Sci., A-2*, **4**, 943 (1966).
19. L. E. Nielsen, *Mechanical Properties of Polymers*, Van Nostrand Reinhold, New York, 1962, p. 252.

Received January 22, 1986

Accepted April 30, 1986